

# Searching for $Z'$ bosons decaying to gluons

Johan Alwall,<sup>1,2</sup> Mazin Khader,<sup>3</sup> Arvind Rajaraman,<sup>3</sup> Daniel Whiteson,<sup>3</sup> and Michael Yen<sup>3</sup>

<sup>1</sup>*Fermi National Accelerator Laboratory, Batavia, IL 60615*

<sup>2</sup>*National Taiwan University, Dept. of Physics, Taipei 10617, Taiwan*

<sup>3</sup>*University of California, Irvine, Irvine, California 92697*

The production and decay of a new heavy vector boson, a chromophilic  $Z'$  vector boson, is described. The chromophilic  $Z'$  couples only to two gluons, but its two-body decays are absent, leading to a dominant decay mode of  $Z' \rightarrow q\bar{q}g$ . The unusual nature of the interaction predicts a cross-section which grows with  $m_{Z'}$  for a fixed coupling and an accompanying gluon with a coupling that rises with its energy. We study the  $t\bar{t}g$  decay mode, proposing distinct reconstruction techniques for the observation of an excess and for the measurement of  $m_{Z'}$ . We estimate the sensitivity of current experimental datasets.

PACS numbers: 12.60.-i, 13.85.Rm, 14.70.Pw, 14.80.-j

## I. INTRODUCTION

Many models of physics beyond the Standard Model predict the existence of new  $U(1)$  gauge factors (e.g. [1–4]). For example, grand unified theories with  $SO(10)$  gauge group naturally have an extra  $U(1)$  gauge factor [5]. Models with extra dimensions at the TeV scale can have extra gauge factors on the hidden brane. String theoretic models usually have extra branes wrapped around higher dimensional cycles, as well as intersecting branes, which can produce new gauge factors [6–15]. In most of these cases, these new  $U(1)$  gauge factors are typically broken either by the Green-Schwarz mechanism or by a charged scalar expectation value, so that the corresponding gauge boson is massive.

If the new sector is completely secluded from the Standard Model, it does not have phenomenological consequences. However, in many of these models, there are massive fields charged under both the hidden and visible gauge groups. Once these fields are integrated out, they can induce couplings between the hidden and visible sectors, which are observable at colliders. This has motivated a great deal of effort in searches for new gauge fields, and in particular new  $Z'$  gauge bosons. If the  $Z'$  boson couples to quarks and leptons, it can produce spectacular signals at colliders as a dijet or dilepton resonance. Current colliders already place stringent constraints on such new bosons which have coupling similar to the Standard Model  $Z$  boson [16–18].

It is however, very plausible that these new gauge bosons have highly suppressed direct couplings to quarks and leptons. If the new gauge boson is from a hidden sector as in string-theoretic models or in models where dark matter arises from a hidden sector, there are typically no tree-level couplings between the Standard Model fermions and the  $Z'$  boson. At the loop level, there can be quantum corrections that mix the  $Z'$  boson with the  $U(1)$  of hypercharge [19–26]. These are called kinetic mixing terms; they are renormalizable and hence unsuppressed by a mass scale. These couplings then induce a coupling between the  $Z'$  boson and the Standard Model

fermions.

However, if there are no fields charged under both hypercharge and the new  $U(1)'$ , these kinetic mixing terms are absent. In this case, the leading interactions between the hidden sector and the Standard Model will come from bifundamental fields charged under  $U(1)'$  and either  $SU(2)$  or  $SU(3)$ . Once these fields are integrated out, there will be new couplings induced between the hidden sector and the gauge bosons of the visible sector which are of the form  $Z'G^2$ , where  $G$  is a field strength either of  $SU(2)$  or  $SU(3)$ .

In this paper, we shall consider the case where the  $Z'$  boson is coupled to the  $SU(3)$  field strength (the case where the coupling is only to the  $SU(2)$  field strength was considered in [28]). We shall refer to these as chromophilic  $Z'$  bosons. We shall discuss the current constraints on such models and possible searches for these models in current experimental collider datasets. We shall be interested to see if this model can be discovered at the Tevatron or the LHC.

Specifically, we will consider a hidden sector consisting of a  $U(1)$  theory broken by an abelian Higgs model. The physical spectrum will then have one massive gauge boson which we denote as  $Z'$ . This sector is coupled to the Standard Model by mediator fields  $\psi$  charged under the  $SU(3)$  of the Standard Model as well as the hidden sector  $U(1)$ . The resulting operators will depend on whether the  $Z'$  boson is a vector or a pseudovector. Motivated by string-theoretic models, we consider the case where  $Z'$  boson is a pseudovector. For an on-shell  $Z'$  boson, the only relevant operator is then [28]

$$\mathcal{L}_{int} = g\epsilon_{\mu\nu\rho\sigma}Z'^{\mu}G^{\nu\rho}\partial_{\alpha}G_{\alpha\sigma} \quad (1)$$

where  $g$  has dimensions of  $\text{mass}^{-2}$ . We aim to find the sensitivity of current experiments as a function of  $Z'$  boson mass and the coupling  $g$ .

Despite the  $Z'$ -gluon-gluon vertex, the chromophilic  $Z'$  boson has no two-body decays. This is because the Landau-Yang theorem [29] prevents a massive gauge boson from decaying to two massless gauge bosons. The only possible decays are three-body decays; the  $Z'$  boson

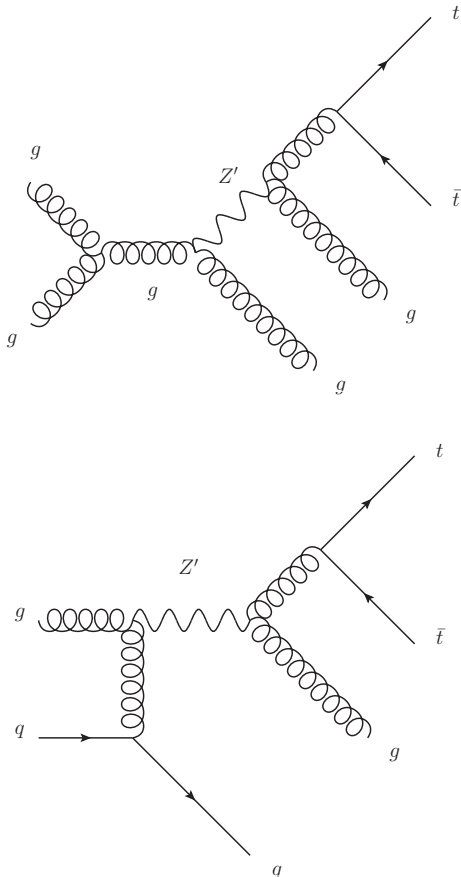


FIG. 1: Diagram for  $Z'g$  (top) or  $Z'q$  (bottom) production followed by  $Z' \rightarrow gg^* \rightarrow g\bar{t}t$  decay giving a  $t\bar{t}gg$  (top) or  $t\bar{t}gq$  (bottom) final state.

can decay to two quarks and a gluon through an off-shell gluon (we found by explicit calculation that the  $Z'$  boson decay to three gluons also vanishes). Furthermore, the  $Z'$  boson is not produced directly in the process  $gg \rightarrow Z'$  for the same reason.

The leading production process is through the process  $q\bar{q} \rightarrow qZ'$  or  $gg \rightarrow gZ'$  through an off shell gluon, followed by the decay  $Z' \rightarrow q\bar{q}g$ . This leads to a  $(q\bar{q}qg$  or  $q\bar{q}gg)$  final state; if the  $q\bar{q}$  pair are light, it gives a four-jet final state which is challenging to see over the large multi-jet background. The usual constraints on  $Z'$  models from dilepton and dijet final states therefore do not apply to this model, which would appear instead in events with four jets.

To extract the signal from the large background, we will look at signal events with heavy flavor. In this paper, we focus on the decay  $Z' \rightarrow g\bar{t}t$  (see Figure 1), which gives a final state of  $t\bar{t} + 2$  jets. We will be aided by the fact that we can require the two heavy quarks along with one of the other jets to reconstruct to the  $Z'$  resonance ( $t\bar{t}j$ ). This final state signature,  $t\bar{t} + 2$  jets, with a reso-

TABLE I: Acceptance of the event selection for  $Z' + j$  production and the dominant background, SM  $t\bar{t} + 2j$ . Statistical uncertainty is approximately 1%.

	Acceptance	
	Tevatron $p\bar{p}$ , 1.96 TeV	LHC $pp$ , 7 TeV
SM $t\bar{t} + 1j$	5%	11%
$Z' + j$ (400 GeV)	7%	9%
$Z' + j$ (500 GeV)	9%	8%
$Z' + j$ (600 GeV)	11%	9%
$Z' + j$ (700 GeV)	11%	10%
$Z' + j$ (800 GeV)	12%	10%
$Z' + j$ (900 GeV)	12%	11%
$Z' + j$ (1000 GeV)	12%	11%

nance in  $t\bar{t}j$  has not yet been experimentally explored.

## II. SELECTION AND BACKGROUNDS

The event selection roughly follows the standard selection for  $t\bar{t} \rightarrow \ell + \text{jets}$  analyses [33, 34] except that we require a fifth jet. Briefly, we require:

- exactly one electron or muon, with  $p_T > 20$  GeV and  $|\eta| < 2.5$
- at least five jets, each with  $p_T > 20$  GeV and  $|\eta| < 2.5$
- at least 20 GeV of missing transverse momentum
- at least one  $b$ -tagged jet

The dominant Standard Model background is  $t\bar{t}$  production with additional jets from initial- or final-state radiation. At the Tevatron (LHC),  $W + \text{jets}$  contributes 25% (10%). In this study, we consider only the  $t\bar{t}$  background.

Both the signal and background events are generated with MADGRAPH 5 [30], while top-quark and  $W$ -boson decay, showering and hadronization are performed by PYTHIA 6.4 [31]. The parametric detector simulation program PGS [32] is tuned for Tevatron or ATLAS as appropriate.

The expected background levels are calculated using the NLO cross-section [35] for  $t\bar{t} + j$  production, acceptance calculated with simulated events, and a luminosity of  $8 \text{ fb}^{-1}$  ( $5 \text{ fb}^{-1}$ ) for the Tevatron (LHC). A 10% normalization uncertainty is used. The acceptance for  $Z'q$  and  $Z'g$  production is calculated using simulated events. Table I shows the acceptances of signal and background for both datasets.

## III. RECONSTRUCTION AND SENSITIVITY

Events are reconstructed according to the  $t\bar{t}$  hypothesis. The neutrino transverse momentum is taken from the

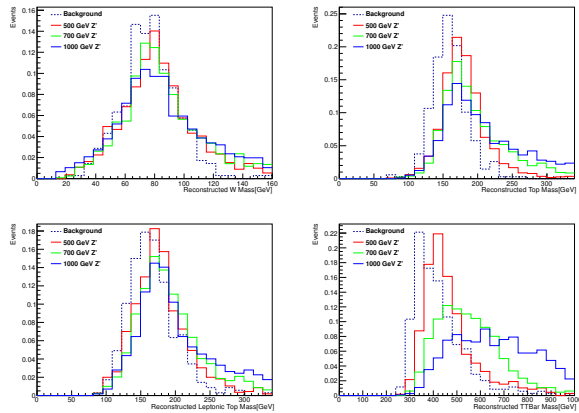


FIG. 2: Distribution at the Tevatron of  $m_{qq'}$ ,  $m_{qq'b}$ ,  $m_{\ell\nu b'}$ , and  $m_{t\bar{t}}$  for the dominant SM background of  $t\bar{t}$ +jets and for two choices of  $Z'$  signal.

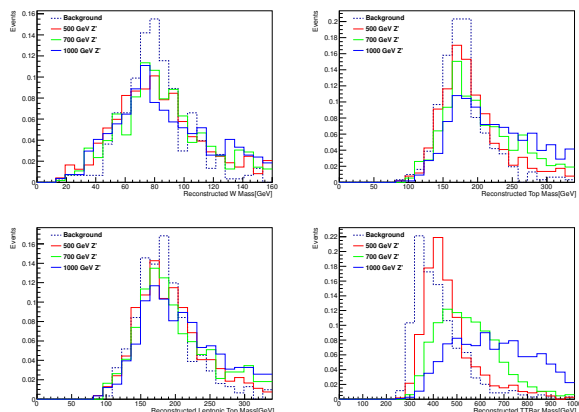


FIG. 3: Distribution at the LHC of  $m_{qq'}$ ,  $m_{qq'b}$ ,  $m_{\ell\nu b'}$ , and  $m_{t\bar{t}}$  for the dominant SM background of  $t\bar{t}$ +jets and for two choices of  $Z'$  signal.

missing transverse momentum; the longitudinal component is set to the smallest value which gives  $(p_\ell + p_\nu)^2 = m_W^2$ . The jets from hadronic  $W \rightarrow qq'$  decay and the two  $b$ -quarks are identified by selecting the jets which minimize the function:

$$\chi^2 = \frac{(m_{qq'} - m_W)^2}{\sigma_{qq'}^2} + \frac{(m_{qq'b} - m_t)^2}{\sigma_{qq'b}^2} + \frac{(m_{\ell\nu b'} - m_t)^2}{\sigma_{\ell\nu b'}^2}$$

where the denominator  $\sigma_{qq'}$ ,  $\sigma_{qq'b}$ ,  $\sigma_{\ell\nu b}$  values which describe the resolution of each mass term are extracted from simulated events. All jets which satisfy the  $p_T$  and  $\eta$  requirements above are considered. Distributions of reconstructed  $W$  boson and top quark candidate masses are shown in Figures 2 and 3 and demonstrate that the reconstruction accurately identifies the  $W$ -boson and top-quark decays.

The mass of the candidate  $Z' \rightarrow t\bar{t}j$  is reconstructed

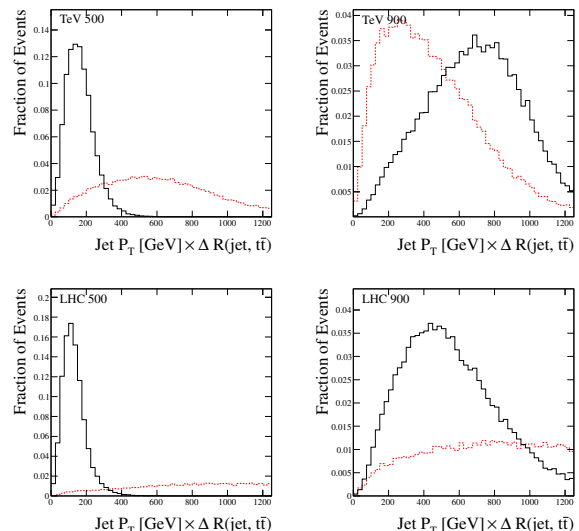


FIG. 4: Distribution of  $\Delta R(jet, t\bar{t}) \times P_T^h$  for jets from the initial state (red, dashed) compared to the additional jet in  $Z' \rightarrow t\bar{t}j$  decays (black, solid). Top row is Tevatron; bottom row is LHC. Left column is  $m_{Z'} = 500$  GeV; right column is  $m_{Z'} = 900$  GeV.

by selecting an additional jet not included in the  $t\bar{t}$  assignment. With the exception of high-mass ( $m_{Z'} > 700$  GeV) cases at the Tevatron, the additional jet from  $Z'$  decay tends to have smaller transverse momentum than the associated jet in  $Z' + g$  or  $Z' + q$  production. In addition, with the same exception, the additional jet from  $Z'$  decay tends to be close to the  $t\bar{t}$  system in angular space, see Figure 4. This is due to eq. (1), which gives an enhanced coupling to highly virtual gluons and corresponding large invariant mass of the  $t\bar{t}$  system, leaving the remaining jet with a relatively small momentum. In the same way, the associated jet in the  $Z' + j$  production is preferentially at large invariant mass with the  $Z'$ , if allowed by the parton luminosities.

We therefore reconstruct the  $Z'$  mass,  $m_{t\bar{t}j}$  using the jet with the smallest value of  $\Delta R(j, t\bar{t}) \times P_T^j$  (the ‘near jet’), as well as the combination  $t\bar{t}j_{\text{far}}$  with the jet with the largest value of  $\Delta R(j, t\bar{t}) \times P_T^j$  (the ‘far jet’) as shown in Figures 5 and 6). As expected, with the exception of the high mass ( $m_{Z'} > 700$  GeV) case at the Tevatron, the near jet gives the most faithful reconstruction of the  $Z'$  mass, while the far jet gives the best signal-background discrimination.

To extract the most likely value of the signal cross section, a binned maximum likelihood fit is used in the  $m_{t\bar{t}j}$  variable, floating the background rate within uncertainties. Both near- and far-jet masses are considered. The signal and background rates are fit simultaneously. The  $\text{CL}_s$  method [36] is used to set 95% cross-section upper limits. The median expected upper limit is extracted in the background-only hypothesis, see Figures 7 and 8.

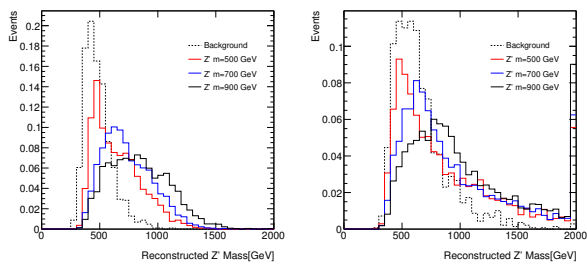


FIG. 5: Distribution of reconstructed  $Z'$  candidate mass ( $m_{t\bar{t}j}$ ) for the dominant SM background of  $t\bar{t}+jets$  and for three choices of  $Z'$  signal, using the ‘near jet’ as defined in the text. Overflow events are included in the last bin. Left is Tevatron, right is LHC.

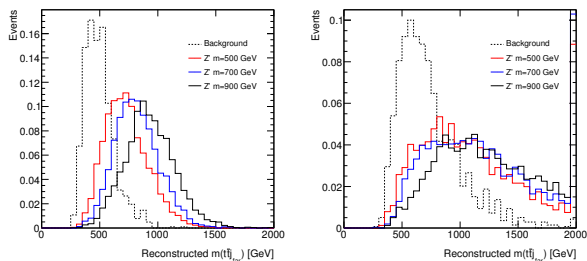


FIG. 6: Distribution of the mass of the  $t\bar{t}j_{far}$  system ( $m_{t\bar{t}j_{far}}$ ) for the dominant SM background of  $t\bar{t}+jets$  and for three choices of  $Z'$  signal, using the ‘far jet’ as defined in the text. Overflow events are included in the last bin. Left is Tevatron, right is LHC.

The far-jet mass gives superior expected exclusion limits.

The Tevatron dataset can exclude  $Z' + j$  production at the level of 10 – 100 fb in the mass range of  $m_{Z'} = 400 - 1000$  TeV. The LHC limits are expected to be weaker, due to the larger SM  $t\bar{t}$  backgrounds. However, the expected cross-section is also larger at the LHC. This becomes clear when the limits are expressed in the plane of  $m_{Z'}$  vs coupling  $g$ , assuming  $\sigma(g) \propto g^2$ .

#### IV. CONCLUSIONS

We have introduced a model for a new heavy vector boson  $Z'$ , which couples only to gluons, but may only

decay via three-body decays as  $Z' \rightarrow q\bar{q}g$ . This model has the additional peculiar feature of a hard associated jet from the initial state. In the case of top-quark decays, the signature is a resonance in  $t\bar{t} + j$  with an associated hard jet, which has not yet been experimentally explored and to which current experimental datasets have sensitivity. We proposed two reconstruction techniques, one using a ‘far’ jet to establish the presence of a signal and one using a ‘near’ jet to perform mass reconstruction in the case of an excess.

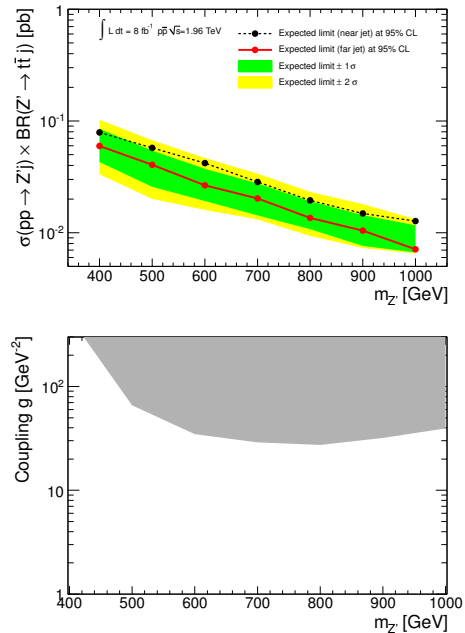


FIG. 7: For Tevatron: top, expected upper limits on the production of  $Z' + j$  at 95% confidence level, as a function of  $Z'$  mass; bottom, expected exclusion region in  $m_{Z'}$  and the coupling, assuming the cross section has a quadratic dependence on the coupling.

#### V. ACKNOWLEDGEMENTS

We thank J. Kumar and D. Yaylali for useful conversations. DW, MK and MY are supported by grants from the Department of Energy Office of Science and by the Alfred P. Sloan Foundation. AR is supported in part by NSF Grant No. PHY-0653656. JA is supported by NTU Grant number 10R1004022.

[1] A. Leike, Phys. Rept. **317**, 143 (1999) [arXiv:hep-ph/9805494].  
 [2] T. G. Rizzo, arXiv:hep-ph/0610104.  
 [3] P. Langacker, Rev. Mod. Phys. **81**, 1199 (2009) [arXiv:0801.1345 [hep-ph]].  
 [4] P. Nath *et al.*, Nucl. Phys. Proc. Suppl. **200-202**, 185

(2010) [arXiv:1001.2693 [hep-ph]].  
 [5] G. G. Ross, *Reading, Usa: Benjamin/cummings (1984) 497 P. (Frontiers In Physics, 60)*  
 [6] R. Blumenhagen, L. Goerlich, B. Kors and D. Lust, Fortsch. Phys. **49**, 591 (2001) [arXiv:hep-th/0010198].  
 [7] M. Cvetič, G. Shiu and A. M. Uranga, “Chiral

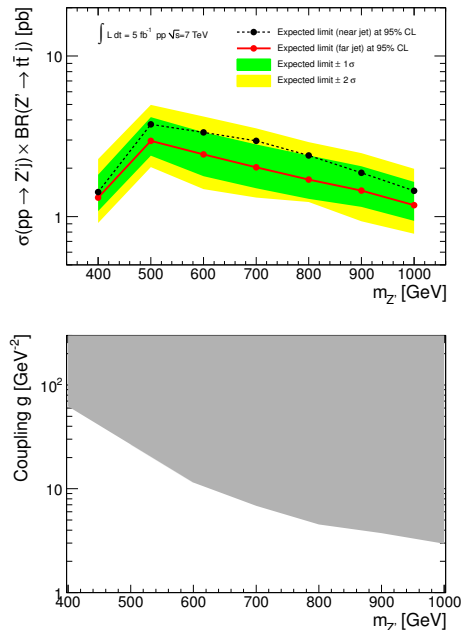


FIG. 8: For LHC: top, expected upper limits on the production of  $Z' + j$  at 95% confidence level, as a function of  $Z'$  mass; bottom, expected exclusion region in  $m_{Z'}$  and the coupling, assuming the cross section has a quadratic dependence on the coupling.

four-dimensional  $N=1$  supersymmetric type 2A orientifolds from Nucl. Phys. B **615**, 3 (2001) [arXiv:hep-th/0107166].

- [8] M. Cvetič, P. Langacker and G. Shiu, “A Three family standard - like orientifold model: Yukawa couplings and Nucl. Phys. B **642**, 139 (2002) [arXiv:hep-th/0206115].
- [9] A. M. Uranga, “Chiral four-dimensional string compactifications with intersecting Class. Quant. Grav. **20**, S373 (2003) [arXiv:hep-th/0301032].
- [10] M. Cvetič, P. Langacker, T. j. Li and T. Liu, Nucl. Phys. B **709**, 241 (2005) [arXiv:hep-th/0407178].
- [11] F. Marchesano and G. Shiu, Phys. Rev. D **71**, 011701 (2005) [arXiv:hep-th/0408059].
- [12] M. Cvetič and T. Liu, “Supersymmetric standard models, flux compactification and moduli Phys. Lett. B **610**, 122 (2005) [arXiv:hep-th/0409032].
- [13] J. Kumar and J. D. Wells, JHEP **0509**, 067 (2005) [arXiv:hep-th/0506252].
- [14] J. Kumar, A. Rajaraman and J. D. Wells, Phys. Rev. D **77**, 066011 (2008) [arXiv:0707.3488 [hep-ph]].
- [15] M. R. Douglas and W. Taylor, JHEP **0701**, 031 (2007) [arXiv:hep-th/0606109].
- [16] J. Alcaraz *et al.* [ ALEPH and DELPHI and L3 and OPAL and LEP Electroweak Working Group Collaborations ], [hep-ex/0612034].
- [17] M. Jaffre [CDF and D0 Collaboration], “Search for high mass resonances in dilepton, dijet and diboson final states PoS E **PS-HEP2009**, 244 (2009) [arXiv:0909.2979 [hep-ex]].
- [18] S. Chatrchyan *et al.* [CMS Collaboration], “Search for Resonances in the Dilepton Mass Distribution in  $pp$  Collisions JHEP **1105**, 093 (2011) [arXiv:1103.0981 [hep-ex]].
- [19] B. Holdom, Phys. Lett. B **166**, 196 (1986).
- [20] F. del Aguila, M. Masip and M. Perez-Victoria, Nucl. Phys. B **456**, 531 (1995) [arXiv:hep-ph/9507455].
- [21] K. R. Dienes, C. F. Kolda and J. March-Russell, Nucl. Phys. B **492**, 104 (1997) [arXiv:hep-ph/9610479].
- [22] J. Kumar and J. D. Wells, Phys. Rev. D **74**, 115017 (2006) [arXiv:hep-ph/0606183].
- [23] D. Feldman, Z. Liu and P. Nath, “The Stueckelberg  $Z$  Prime at the LHC: Discovery Potential, Signature JHEP **0611**, 007 (2006) [arXiv:hep-ph/0606294].
- [24] W. F. Chang, J. N. Ng and J. M. S. Wu, Phys. Rev. D **74**, 095005 (2006) [Erratum-ibid. D **79**, 039902 (2009)] [arXiv:hep-ph/0608068].
- [25] W. F. S. Chang, J. N. Ng and J. M. S. Wu, Phys. Rev. D **75**, 115016 (2007) [arXiv:hep-ph/0701254].
- [26] D. Feldman, Z. Liu and P. Nath, “The Stueckelberg  $Z$ -prime Extension with Kinetic Mixing and Milli-Charged Phys. Rev. D **75**, 115001 (2007) [arXiv:hep-ph/0702123].
- [27] P. Anastasopoulos, M. Bianchi, E. Dudas and E. Kiritsis, JHEP **0611**, 057 (2006) [arXiv:hep-th/0605225].
- [28] J. Bramante, R. S. Hundi, J. Kumar, A. Rajaraman and D. Yaylali, Phys. Rev. D **84**, 115018 (2011) [arXiv:1106.3819 [hep-ph]].
- [29] L. D. Landau, Dokl. Akad. Nauk., USSR **60**, 207 (1948) C. N. Yang, Phys. Rev. **77**, 242 (1950)
- [30] J. Alwall *et al.* JHEP **1106**, 128 (2011).
- [31] T. Sjostrand, S. Mrenna and P. Z. Skands, JHEP **0605**, 026 (2006).
- [32] J. Conway <http://www.physics.ucdavis.edu/conway/research/software/pgs/pgs.html>
- [33] CDF Collaboration, Phys. Rev. Lett. **97**, 082004 (2006); D0 Collaboration, Phys. Rev. **D76**, 092007 (2007).
- [34] ATLAS Collaboration, Eur. Phys. J. C **71** (2011) 1577; CMS Collaboration, Eur. Phys. J. C **71** (2011) 1721.
- [35] M. Aliev *et al.*, HATHOR HAdronic Top and Heavy quarks crOSS section calculator, arXiv:1007.1327 [hep-ph].
- [36] A. Read, J. Phys. G: Nucl. Part. Phys. **28** (2002) 2693; T. Junk, Nucl. Instr. Meth. A **434** (1999) 435.